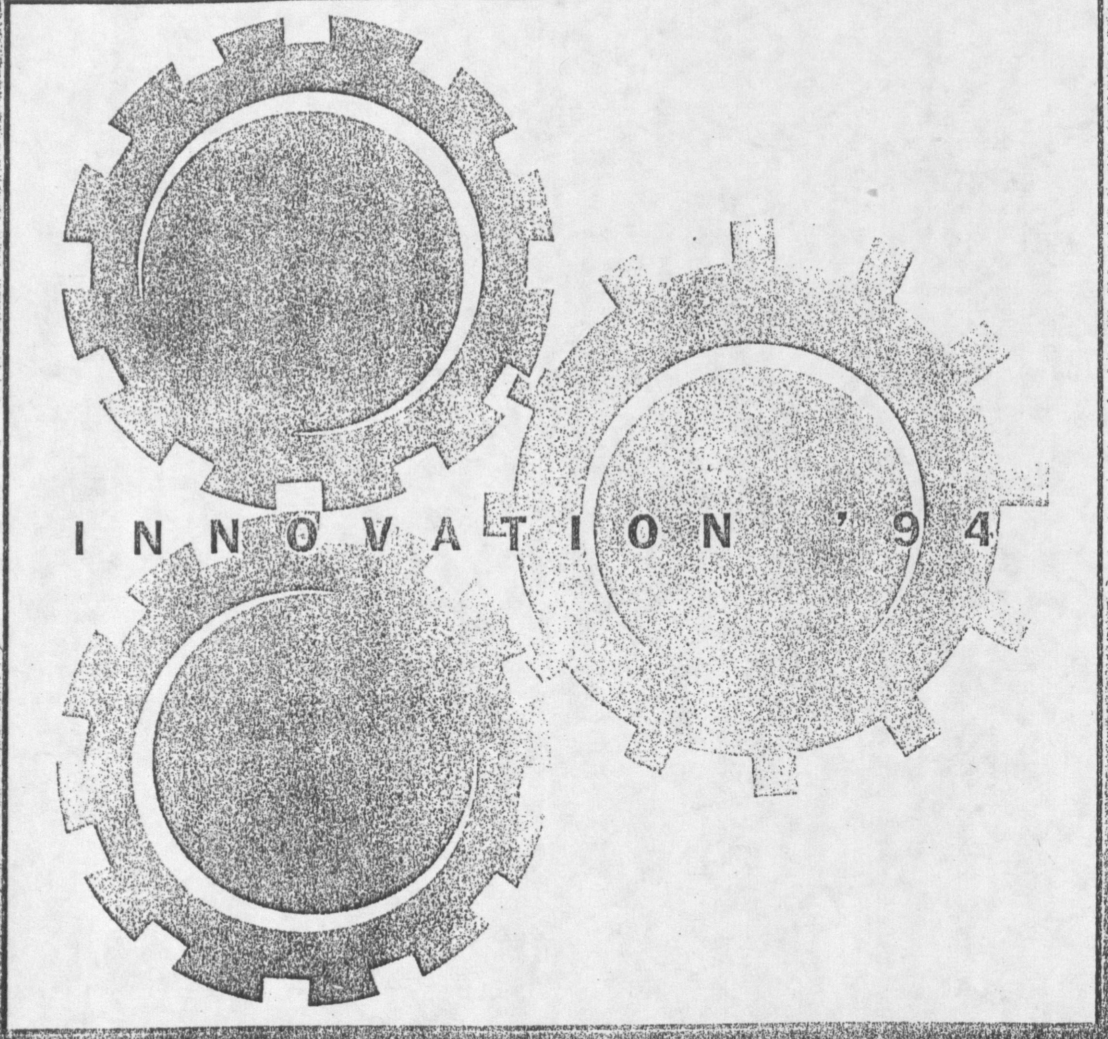

First Meeting of the Society of Magnetic Resonance

Printed Program

Guest Editors
Laurence P Clarke, PhD
Richard L Ehman, MD
Norbert J Pelc, ScD
Jeffrey S Ross, MD

Journal of Magnetic Resonance Imaging
Published by the Society of Magnetic Resonance

A supplement to JMRI January/February 1994 Issue, Volume 4(P)

creases imaging time and the available number of phases of cine images.

226 • 11:30 AM

Correction for Planar Rigid-Body Movements during MRI

ML Wood, PL Stanchev, MJ Shivji
Department of Imaging Research, University of Toronto, Sunnybrook Health Science Centre, Toronto, Ontario, Canada

Purpose: We demonstrate a method of correcting MR images for rigid-body motion in the imaging plane.
Methods: Two sets of k-space data are acquired by using a pulse sequence that interchanges the phase-encoding and frequency-encoding directions. These data provide 1D projections onto both directions of the imaging plane, from which displacements are estimated. Translation alters the center of 1D projections, while rotation alters their width and shape. The k-space data are phase shifted to correct for translation. Data to be corrected similarly for rotation are copied to an empty array the same size as k space. This array is given Hermitian symmetry by synthesizing the opposite half of k space and adding it to the array. The data are transformed to the spatial domain, rotated, transformed back to k space, and then added to a new array. After all of the data have been rotated as desired, a complementary step is to replace corrupted data with any corresponding uncorrupted data from the other side of k space. Finally, the two sets of corrected data are combined and then reconstructed into an image.
Results: It was possible to measure the width of 1D projections for every k_y. The correction reduced the ghosts and blurring in a transverse image of a patient nodding his head in the transverse plane.
Conclusion: Rigid-body movements of certain structures can be detected from k-space MR data, which then can be corrected to reduce the associated ghosts and blurring.

227 • 11:42 AM

Nonsusceptibility Effects of Metallic Implants in MR Imaging

CR Camacho, RM Henkelman, DB Plewes
University of Toronto, North York, Ontario, Canada

Purpose: Local artifacts produced by nonferromagnetic metal implants degrade MR image quality. In this study, we investigated and proposed corrections for artifacts resulting from RF-induced eddy currents in the metal.
Methods: A circular copper wire loop was used to provide a simple eddy-current pathway with minimal susceptibility effects. The loop was placed in an $MnCl_2$ solution and imaged by using various clinical pulse sequences in a 1.5-T imager with both linearly and circularly polarized RF coils. A change in the orientation and location of the copper loop allowed independent investigation of eddy currents induced by either RF pulses or field gradients. The effects of RF eddy currents on the transmit/receive sensitivity of the RF coil were quantified by analyzing the variation in MR signal as a function of transmit gain to the RF coil. These effects were also simulated numerically for both RF polarizations.
Results: We observed no artifacts due to field gradients. However, RF-induced eddy currents produced substantial artifacts in the vicinity of the loop. These artifacts were shown to be caused by the spatial variation of the transmit/receive sensitivity of the RF coil that resulted from the RF eddy currents. Simulations of this variation agreed with experimentally obtained values, which confirmed our understanding of its cause.
Conclusion: This study explains the basis of RF eddy-current artifacts that exist whenever good conductors are imaged. An understanding of this basis suggests several methods for artifact minimization. For example, GRE sequences are less sensitive than spin-echo to RF transmit nonuniformity and show reduced artifacts.

228 • 11:54 AM

Excitation of a 1-mm-Diameter Beam with Response Modulated Excitation

TJ Wieczorek, JD Pearlman
Beth Israel Hospital, Boston, MA

Purpose: To confine magnetic excitation to a 1-mm-diameter beam deep inside a target.
Methods: A response modulated excitation (RME) algorithm was implemented to calculate an RF pulse and gradient trajectory designed to excite a beam of magnetization with a diameter of 1 mm and an axial length of 5 mm. A square beam cross section was prescribed to maximize the sharpness of the cutoff between the beam and the background. The RME algorithm was fine-tuned with an FFT-based simulation of magnetization excited by the prescribed RF and gradient waveforms. An analog filter was used to minimize stray excitation in one direction perpendicular to the beam. Experiments were performed in a water phantom with a Siemens 1.5-T EPI scanner using a blipped EPI excitation with an excitation time of 8 msec.
Results: A 1-mm beam was obtained with signal dropoff to less than 12% of the peak height over a distance of 1 mm in either of two directions perpendicular to the beam axis. Mean signal magnitude outside the beam in a 65-mm square was .00151, with a standard deviation of .00628, compared with a normalized magnitude of 1 inside the beam.
Conclusions: Magnetization may be confined so that MR signal is obtained from a precisely localized region deep within an excitation target. Confinement of magnetization to narrow beams opens up the possibility for precise M-mode imaging of valve motion in the human heart, small field-of-view imaging without aliasing, and magnetic "tagging" of small moving structures.

Tuesday Morning • Morrocco Room
Papers 231–237

SPECTROSCOPY II: Brain

MODERATORS: F Arias-Mendoza, MD, PhD
IR Young, PhD

231 • 10:30 AM

Measurement of Metabolite Concentrations and T2 in Brain with Proton MRS: Increased Choline T2 of Meningiomas

M Lowry, DJ Manton, SJ Blackband, A Horsman
Centre for MRI, Hull Royal Infirmary, Hull, England

Purpose: To obtain estimates for T1, T2, and concentrations of choline, creatine, and N-acetylaspartate (NAA) in normal brain and meningiomas.
Methods: Thirty volunteers and 8 patients were examined with a GE 1.5-T Signa. Voxels (8 mL) were placed in white matter, gray matter, cerebellum, and meningioma. Spectra were acquired by using STEAM with a TR of 0.8–10 seconds and TE of 30–272 msec. Water reference spectra were also acquired for each TE. Concentrations were calculated by using the method of Barker et al (1).
Results: Compared with white matter, meningiomas were characterized by the absence of NAA, increased choline/creatine area ratio (5.6 ± 3.2 vs 1.3 ± 0.2, mean ± SD), and the presence of alanine in spectra acquired at TE = 272 msec. Values of T2 for choline, creatine, and NAA in white matter were 223 msec ± 96, 154 msec ± 30, and 447 msec ± 114, respectively. The T2 of NAA was significantly less in gray matter (320 msec ± 52, $P < .05$) and cerebellum (335 msec ± 75, $P < .05$), while choline T2 of meningiomas (381 msec ± 66) was greater than that in any region of normal brain ($P < .05$). Calculated white matter metabolite concentrations were 3.3 μmol/g ± 0.7, 13.2 μmol/g ± 1.9, and 13.4 μmol/g ± 1.4 fresh weight for choline, creatine, and NAA, respectively. Choline and creatine concentrations in meningiomas were 4.5 μmol/g ± 1.1 and 9.4 μmol/g ± 2.7, respectively.

(52.) *Wood M., Stanchev P., Shivji M., "Correction for Planar Rigid-Body Movements during MRI", ***JMRI*** 1994, 4(P): 62.